Food and Bioprocess Technology (2024) 17:1752–1764
https://doi.org/10.1007/s11947-023-03226-7

RESEARCH

Evaluation of Hydrothermal and Alkaline Pretreatment Routes for Xylooligosaccharides Production from Sugar Cane Bagasse Using Different Combinations of Recombinant Enzymes

Caio Cesar de Mello Capetti[1] · Vanessa de Oliveira Arnoldi Pellegrini[1] · Milena Moreira Vacilotto[1] · Antonio Aprigio da Silva Curvelo[2] · Maurício Falvo[1] · Francisco Eduardo Gontijo Guimaraes[1] · Ornella M. Ontañon[3,4] · Eleonora Campos[3,4] · Igor Polikarpov[1]

Received: 30 April 2023 / Accepted: 6 October 2023 / Published online: 18 October 2023

Abstract

Xylan is the most abundant constituent of hemicellulose fraction of lignocellulosic biomass. Short xylooligosaccharides (XOS), obtained via xylan hydrolysis, have well-known prebiotic and antioxidant properties that are beneficial for human and animal health. In this study, two alternative pretreatment strategies (alkali and hydrothermal) and three different enzymes were applied for enzymatic XOS production from sugarcane bagasse. The enzymatic hydrolysis was performed with nine different combinations of recombinant endo-xylanases from GH11 and GH10 families and GH11 xylobiohydrolase. Hydrothermal pretreatment followed by optimized enzymatic hydrolysis yielded up to 96 ± 1 mg of XOS per gram of initial biomass, whereas enzymatic hydrolysis of alkali-pretreated sugarcane bagasse rendered around 47.6 ± 0.2 mg/g. For both alkali and hydrothermal routes, the maximum yields of short-length XOS were obtained using the GH10 xylanase alone. Furthermore, differences in XOS profiles obtained by controlled mixtures of the enzymes have been evaluated. For both routes, the best yields of short-length XOS were obtained using the GH10 xylanase alone, which is consistent with the notion that sugarcane xylan substitutions partially hinder GH11 xylanase activity. The results presented here show that a green and cost-effective hydrothermal pretreatment path for xylooligosaccharides production, rendered considerably better XOS yields.

Keywords Xylooligosaccharides · Sugarcane bagasse · Xylanases · Hydrothermal pretreatment · Alkali pretreatment

Introduction

Lignocellulosic materials (LCM), such as sugarcane bagasse (SCB), are important and abundant sources of polysaccharides and lignin. In Brazil alone, the world's biggest producer, 654.5 million tons of sugarcane from the 2020/2021 harvest were crushed, yielding 41.3 million tons of sugar and 29.7 billion liters of ethanol, while generating around 230 million tons of solid residues (CONAB, 2021). LCM are mainly composed of cellulose, hemicelluloses, and lignin, playing a fundamental role in the composition of the plant cell wall. Hemicelluloses, which represent around 20 to 35% of plant biomass, comprise heteropolysaccharides such as xylan, for example (Timell, 1967). Xylan has multiple biotechnological applications in the production of biofilms (Alekhina et al., 2014), paper coatings, adhesives (Farhat et al., 2017), and biofuels, to name a few.

Xylan is the second most abundant renewable natural polysaccharide after cellulose. Its backbone consists of D-xylopiranosyl (Xylp) residues covalently bound via β-1,4 linkages. Xylan composition may vary according to plant species, but, in general, it presents side substituents such as α-1,2 linked glucuronic acids (GlcA and MeGlcA) in

✉ Igor Polikarpov
ipolikarpov@ifsc.usp.br

1 Instituto de Física de São Carlos, Universidade de São Paulo, Avenida Trabalhador São-carlense 400, São Carlos, SP 13566-590, Brazil

2 Instituto de Química de São Carlos, Universidade de São Paulo, Avenida Trabalhador São-carlense 400, São Carlos, SP 13566-590, Brazil

3 Instituto de Biotecnología, Los Reseros y N. Repetto, Instituto Nacional de Tecnología Agropecuaria (INTA), Hurlingham B1686, Buenos Aires, CICVyA, Argentina

4 Consejo Nacional de Investigaciones Científicas y Técnicas (CONICET), Ciudad Autónoma de Buenos Aires, Argentina

glucuronoxylans and/or α-1,3 linked arabinofuranosyl residues (Ara*f*) in arabinoxylans (Deutschmann & Dekker, 2012).

Previously, it has been identified that sugarcane contains arabinoglucuronoxylan as the main fraction of its hemicellulose, which may bear L-arabinose decorations mainly at the position 3 of the xylopyranose residues and 4-O-methylglucuronic acid decorations mainly at position 2 (Fig. 1), with Ara*f* substitutions being 3–fivefold more frequent than MeGlcA decorations (Carvalho et al., 2016). Arabinoglucuronoxylan also could be acetylated at positions 2 and 3 (Biely et al., 2016).

It is well established that xylooligosaccharides (XOS), a product of xylan hydrolysis under controlled conditions, have many positive impacts on animal and human health, such as reduction of cholesterol levels, enhancing calcium absorption, lipid metabolism regulation, and diminishing the chances of colon cancer development associated with intestinal activity control, effects that have also been observed with other hemicellulose-originated oligosaccharides (Capetti et al., 2023; Hong et al., 2016). XOS impact on the digestive system, especially short ones, as X2–X4 (Vázquez et al., 2000), is due to their prebiotic effect, i.e., their ability to selectively stimulate the growth of beneficial bacteria, like those of *Bifidobacterium* genus (Singh et al., 2015). Additionally, XOS can also act as antioxidants due to the presence of uronic and ferulic acids in their decorations (Vieira et al., 2020) and as antimicrobials (de Freitas et al., 2019; Hitache et al., 2023), counterbalancing the potential proliferation of pathogenic bacteria, including *Salmonella* (Asahara et al., 2001).

To produce XOS, it is crucial to perform a pretreatment in the biomass to disrupt the lignocellulosic recalcitrant complex. This pretreatment can be chemical, physical, or biological. The main objective is to solubilize the cell wall and to make the polymeric components accessible for further enzymatic hydrolysis. After this, XOS can be obtained by enzymatic hydrolysis. Alkali pretreatments, commonly performed employing sodium hydroxide, potassium hydroxide, ammonium hydroxide, or calcium hydroxide solutions, result mainly in lignin solubilization, deacetylation, and disruption of lignocellulosic complex, allowing for subsequent enzymatic hydrolysis (Yuansah et al., 2023).

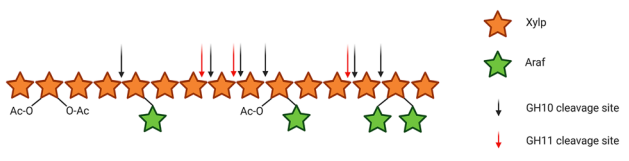

Fig. 1 Schematic representation of sugarcane arabinoglucuronoxylan structure. GH10 and GH11 cleavage sites are indicated with black and red arrows, respectively. Orange stars represent D-xylopyranose (Xyl*p*) residues, while arabinofuranosyl (Ara*f*) decorations are shown as green stars, 4-O-methyl glucuronic acid (MeGlcA) decorations as blue and white square and acetyl groups are represented as "Ac"

Alternatively, hydrothermal pretreatment is a cheap, clean, and effective pretreatment strategy, which relies on pressurized hot water to solubilize hemicellulose from plant biomass (Costa et al., 2023; Espirito Santo et al., 2018; Wang et al., 2012). However, high severity pretreatments can lead to undesirable co-products and inhibitors production (furfural, hydroxymethylfurfural) and to degradation of significant part of xylan into xylose (Yuansah et al., 2023). Therefore, less severe pretreatments are preferable for XOS production. Once xylan is isolated or solubilized, enzymatic hydrolysis can be performed to obtain short-length XOS (de Souza & Kawaguti, 2021; Santibáñez et al., 2021; Yuansah et al., 2023).

Xylanases differ in their specificities and tolerances for xylan decorations, including acetylation. GH10 xylanases are capable of cleaving the xylan main chain if there are two consecutive undecorated xylopyranose residues, whereas xylanases from GH11 family require three consecutive undecorated xylopyranose residues, tolerating Ara*f* decorations in positions − 3, − 2, and + 2 (Capetti et al., 2021). Given the considerable proportion of L-arabinose decorations (about 20% of SCB arabinoxylan; (Campbell et al., 2019)), GH10 xylanases would potentially have more available cleavage sites and therefore should be able to generate a higher number of hydrolytic products.

Furthermore, exo-acting GH11 xylobiohydrolase have been recently discovered in the metagenomic studies of composting microbial consortium (Evangelista et al., 2019; Mello et al., 2017). The detailed molecular mechanism of their activity was recently uncovered (Kadowaki et al., 2021), explaining the structural reasons of why these enzymes, acting from non-reducing ends of xylan chains, liberate xylobiose as a main hydrolytic product (Evangelista et al., 2019; Mello et al., 2017).

Although xylanases are widely applied for enzymatic XOS production (de Souza & Kawaguti, 2021; Yuansah et al., 2023), detailed studies of the differences in hydrolytic product profiles obtained using enzymes from different GH families are scarce (Gufe et al., 2022) and often employ purified xylan as substrate or use combinations of xylanases with accessory enzymes (Malgas et al., 2019). Furthermore, possible synergies between GH10 and GH11 xylanases and GH11 xylobiohydrolases in XOS production from SCB have not been studied as so far. Herein, we set out to compare XOS production using alkali and hydrothermally pretreated sugarcane bagasse. The solid fraction of the alkali-pretreated SCB and both solid and liquid fractions of the hydrothermal pretreated SCB were used to produce XOS. In addition, different possible combinations of GH10 and GH11 xylanases (*Px*Xyn10A, *Px*Xyn11B) and GH11 xylobiohydrolase (MetXyn11) were evaluated, aiming to optimize the mixtures

of the enzymes for elevated yields of short-chain XOS with high prebiotic potential.

Material and Methods

Raw Material

Sugarcane bagasse provided by Raízen (Cosan Group, Piracicaba, SP, Brazil) was used for XOS production. The substrate was washed with water at a temperature of 50 °C to remove remaining sugars and impurities. Next, SCB samples were dried at 40 °C until humidity drop below 10%. Finally, the biomass was milled with a knife mill to approximately 20-mesh and stored in plastic bags at room temperature until used.

Biomass Pretreatment

Alkali pretreatment was performed with 1% w/v NaOH solution and the solid/liquor ratio of 1 g of biomass dry mass per 10 mL of pretreatment solution. The mixture was taken to autoclave for 40 min at 120 °C. The solids were recovered via filtration and used for composition analysis and XOS production. The solids were recovered via filtration and used for composition analysis and XOS production. A minute fraction of oligosaccharides was present in the liquid fraction, and therefore it could not be used to produce XOS.

For the hydrothermal pretreatment, we utilized a 1-L Parr reactor, maintaining the solids load at the proportion 1:10 (w/v). The reaction proceeded at 160 °C and 73 psi, for 1 h under 250 RPM mechanical agitation. After the pretreatment was finished, the reactor was inserted in a bucket full of ice. The liquor was then separated from the solids via vacuum filtration. Both liquid and solid fractions were used as substrates for XOS production.

Samples of liquid fractions from both alkali and hydrothermal pretreatments were analyzed via high-performance anion exchange chromatography (HPAEC) in the same conditions as described in "Analytical Methods for Xylooligosaccharides Quantification" in order to assess XOS production from pretreatments alone.

Chemical Characterization of the Biomass

National Renewable Energy Laboratory (NREL, Golden, CO, USA) methodology was used for determination of structural carbohydrates, lignin, ash, and extractives (Sluiter et al., 2008a, b), with adaptations as described and validated by Gouveia et al. (2009).

In brief, prior to chemical characterization and only in non-treated biomass samples, we performed a Soxhlet extraction with 1:1 cyclohexane–ethanol solution under reflux for 8 h. Five cycles of water extraction followed, also for 8 h/cycle. The samples were then dried and weighted, so that a proportion of extractives could be determined.

For quantification of carbohydrates and lignin, the procedure consists of two consecutive hydrolysis steps of the biomass samples. The first hydrolysis was conducted with concentrated acid conditions (H_2SO_4 72%, 7 min at 45 °C). The mixture was diluted to 4% H_2SO_4 and then taken to autoclave for 30 min at 121 °C, condition under which the second hydrolysis took place. The samples were then filtrated to separate soluble and insoluble fractions.

The resulting liquids were analyzed in a high-performance liquid chromatography system (HPLC), responsible for quantifying compounds that make up cellulosic and hemicellulosic fractions, such as glucose, xylose, acetic acid, formic acid, and arabinose.

The HPLC chromatography system is equipped with a refraction index detector, UV–VIS detector and an Aminex column (HPX-87H, 300 × 7.8 mm, Bio-Rad, USA). The eluent used was sulfuric acid 5 mM, with a flux of 0.6 mL/min for 60 min. Arabinose, glucose, xylose, and acetic acid solutions were utilized as standards. Soluble lignin fraction was quantified via spectrophotometry measurements at 280 nm wavelength (Sluiter et al., 2008b).

Physical Characterization of the Biomass

Untreated and pretreated biomass samples had their physical properties assessed through three techniques: confocal laser scanning microscopy, X-ray diffraction, and nuclear magnetic resonance.

Confocal Laser Scanning Microscopy

The distribution of lignin in the cell walls of treated and untreated sugarcane bagasse was assessed with confocal laser scanning microscopy (CLSM) technique. A Zeiss LSM 780 confocal microscope with a plan-apochromat objective lens (20 ×) and a coherent chameleon laser (Ti–Sapphire) for two-photon excitation was used to measure lignin fluorescence. Prior to microscopic analysis, water was added to samples to form a suspension, which was the set on cover slides. Three scans were performed to form each image, which contains 1024 × 1024 pixels with a lateral resolution of about 300 nm.

Space–Spectral Mapping Analysis

Deeper quantitative analysis of CLSM images was carried out through the spectral space mapping method (Forgy, 1965; Ma et al., 2010). With this technique, each pixel is individually characterized and assigned to clusters using the *K*-means method, which has been previously described

(Pellegrini et al., 2022). Then, cluster population sizes are evaluated relative to the total number of pixels in the image and average *K*-spectra are obtained and normalized to be graphically displayed.

X-Ray Powder Diffraction

X-ray powder diffraction was used to obtain crystallinity indices (CrIs) and crystallite widths of the biomass cellulosic fraction. Data collection was carried out in ambient temperature, in a Rigaku Rotaflex diffractometer model RU200B (Tokyo, Japan) equipped with a graphite monochromator, set at 45 kV and 36 mA. Scan range was from 5° to 50°, with 0.05° steps, using copper X-ray radiation at 1.54 Å and 15 s exposure time. Calculation of CrIs and crystallite widths were performed with empirical method described by Segal et al. (1959) and Scherrer equation (Monshi et al., 2012; Scherrer, 1912), respectively.

Enzymatic Hydrolysis

To obtain well-defined XOS mixtures from xylan, GH10 and GH11 xylanases (*Px*Xyn10A (GenBank: WP_053782506.1) and *Px*Xyn11B (GenBank: WP_053781844.1)), respectively, both from *Paenibacillus xylanivorans* (Ghio et al., 2018) and GH11 exo-β- xylobiohydrolase (MetXyn11 (GenBank: ATY75129.1)), identified in a metatranscriptome analysis of a consortia of sugarcane bagasse compost-derived microbes (Evangelista et al., 2019) were utilized alone and in combinations. Heterologous expression and enzyme purification were successfully performed as described in aforementioned works. We have used the solid fraction of the alkali-pretreated SCB and both solid and liquid fractions originating from hydrothermal pretreatment as substrates for XOS production.

Enzymatic hydrolysis using the solid fraction was carried out with the biomass w/v ratio of 2% in phosphate buffer 50 mM at pH 6.0 and 50 °C. Two-milliliter reactions were kept under agitation (1000 RPM) in a ThermoMixer® (Kasvi, Brazil), for 48 h. 33% (v/v) of liquid substrate obtained from hydrothermal pretreatment (SCB-HT-Liq) was used to perform hydrolysis.

Single enzymes were used at 6.25 mg/g of biomass dosages. In addition, searching for possible synergistic effects, *Px*Xyn10A, an endo-xylanase from GH10 family, was supplemented with a GH11 family endo-xylanase *Px*Xyn11B or exo-xylobiohydrolase MetXyn11 in different proportions. Enzymes were used at mass ratios (GH10:GH11) of 3:0; 2:1; 1:1; 1:2, and 0:3.

Nine different enzyme combinations were applied to each of the biomass samples and reactions were performed in duplicates. Given a fact that liquid fraction after alkaline pretreatment contained mostly solubilized lignin fragments, it was not considered for XOS production and only remaining solid fraction was employed for this purpose. Samples without addition of the enzymes (0:0) were used as control groups.

Analytical Methods for Xylooligosaccharides Quantification

After 48 h of enzymatic hydrolysis, samples were boiled at 95 °C for 5 min and centrifuged at 17,000 × *g* for 5 min. Products from enzymatic hydrolysis were analyzed by HPAEC coupled with pulsed amperometric detection using ICS-5000 system (Dionex, Sunnyvale, USA) equipped with a CarboPac PA1 analytical column 250 mm × 2 mm (Dionex, Sunnyvale, USA). Two buffers were utilized to elute the samples. First, sodium hydroxide 100 mM buffer (buffer A) and the second is sodium acetate 500 mM plus sodium hydroxide 100 mM (buffer B). The flux was adjusted to 0.3 mL/min, the temperature was set to 30 °C, the injection volume was 1 µL. Samples were filtered using 0.22-µm filters (Perfectalab, São Paulo, Brazil) prior to injection.

XOS with DP up to 6 in hydrolysates were determined using a calibration curve of X1–X6 standard mixtures (all from Sigma-Aldrich, St. Louis, USA). XOS yields (Y_{XOS}) from solid substrates, in mg per gram of initial biomass, were calculated as follows:

$$Y_{XOS} = [XOS]/[substrate]\ Y_{PT} \quad (1)$$

where substrate concentration ([substrate]) was 2% and Y_{PT}, pretreatment yield, was determined by the relation:

$$Y_{PT} = (\text{mass recovered after pretreatment})/(\text{initial mass}) \quad (2)$$

Here, pretreatment yields were 60% and 65% for alkali and hydrothermal pretreatment, respectively.

Yield of XOS from liquid substrates was calculated as follows:

$$Y_{XOS} = [XOS]/[substrate] \cdot (\text{total liquor volume}) / (\text{initial mass}) \quad (3)$$

In this case, the substrate concentration (*[*substrate*]*) was 33% and the ratio of total liquor volume and initial biomass prior to hydrothermal pretreatment was 16.6 L/g.

Results and Discussion

Chemical Characterization of Biomass

A key process for successful enzymatic hydrolysis is biomass pretreatment, which is responsible for reducing lignocellulosic complex recalcitrance, hence changing plant biomass chemical composition (Rezende et al., 2011). Chemical

characterization of SCB samples prior and after being submitted to alkali or hydrothermal pretreatments were performed and constituents' proportions are given in Fig. 2.

Chemical composition of untreated sugarcane bagasse (SCB) is consistent with previously published data (Espirito Santo et al., 2018; Poletto et al., 2020). Both pretreatments led to removal of extractives.

The lignin content was reduced to 10.7% after alkali pretreatment, which is in agreement with previous studies that employed this method to pretreat LCMs (Rezende et al., 2011; Zhu et al., 2016). Furthermore, no acetyl groups were detected in this sample, as a result of hemicellulose deacetylation due to alkaline pretreatment (Castro et al., 2017; Zhu et al., 2016). A solids recovery of 60% was achieved after alkali pretreatment.

On the other hand, hydrothermal pretreatment, after which we were able to recover 63% of solids, led to a decrease in xylan content from 22.6% in the untreated biomass to 15.6%, similar to what was described by (Espirito Santo et al., 2018). In the latter study, a decrease to 15.8% has been observed. Simultaneously with these changes, the content of cellulose in the pretreated samples increased to 49.5% in SCB-Alk and 47.0% in SCB-HT, as consequence of other components removal. In fact, when corrected by the pretreatment yields, it becomes clear that part of cellulose mass was actually lost in the pretreatment processes.

Furthermore, analysis of the acetyl group presence in each sample shows that xylan present in the alkali-pretreated material is almost completely deacetylated, while only partial xylan deacetylation was provoked by hydrothermal pretreatment. The results are consistent with the mechanisms of pretreatments, since the alkali solution neutralizes acetyl groups fully, whereas hydrothermal pretreatment uses a change in water pKa as a result of increasing temperature, which releases acetyl groups from xylan. This further reduces pH, acting as a catalyst for xylan depolymerization (Ruiz et al., 2013).

Physical Characterization of Biomass

In addition to chemical composition changes, pretreatments also modify physical properties of biomass (Scapini et al., 2021; Wu et al., 2020). To further understand how pretreatments affected lignocellulosics, we recurred to confocal laser scanning microscopy and X-ray powder diffraction experiments to assess crystallinity, average crystallite sizes, and lignin (re)arrangements in biomass samples. These properties are associated to enzymatic hydrolysis efficiency, as models suggest that accessible surface area, the presence of lignin and enzyme diffusion are determining factors for enhanced hydrolysis (Zhang, Ren et al., 2021; Zhang, Han et al., 2021).

Confocal Laser Scanning Microscopy

Confocal laser scanning microscopy (CLSM) of lignin autofluorescence using two-photon excitation is a powerful tool to characterize lignin organization and aggregation and in

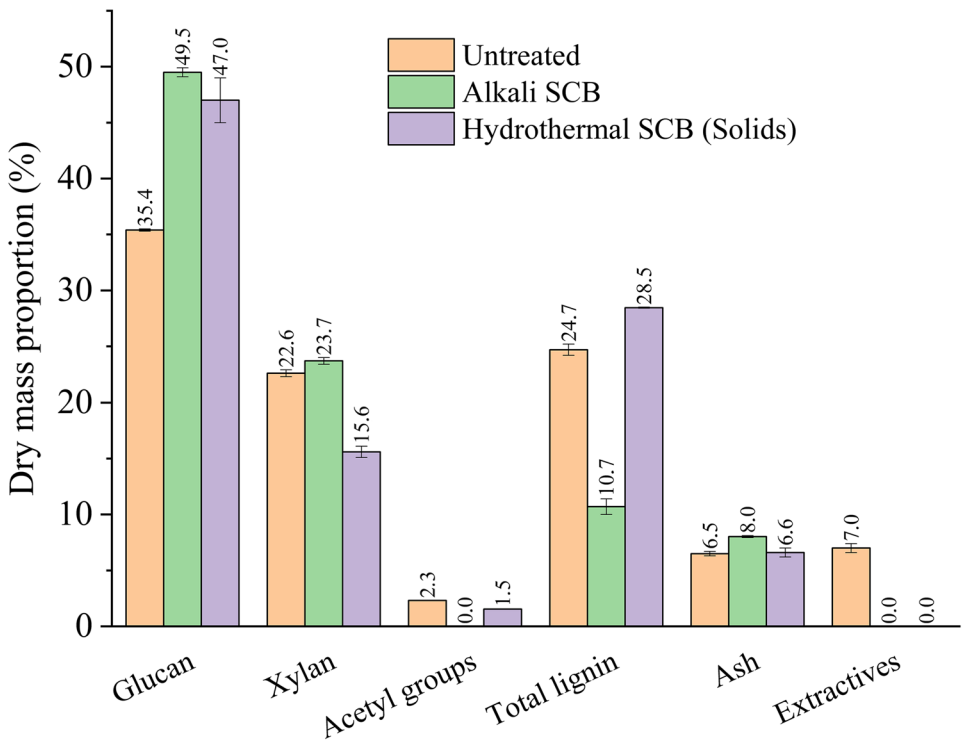

Fig. 2 Chemical composition (% dry basis) of in natura biomass and residual solids after performing two different pretreatments. "Total lignin" comprehends acid soluble lignin and insoluble lignin. IN, in natura or untreated biomass; Alk, alkali-pretreated; HT, hydrothermal pretreated; SCB, sugarcane bagasse. Results are given as the mean of duplicates and, the errors, as the standard deviation ($n = 2$). N/D, not detected

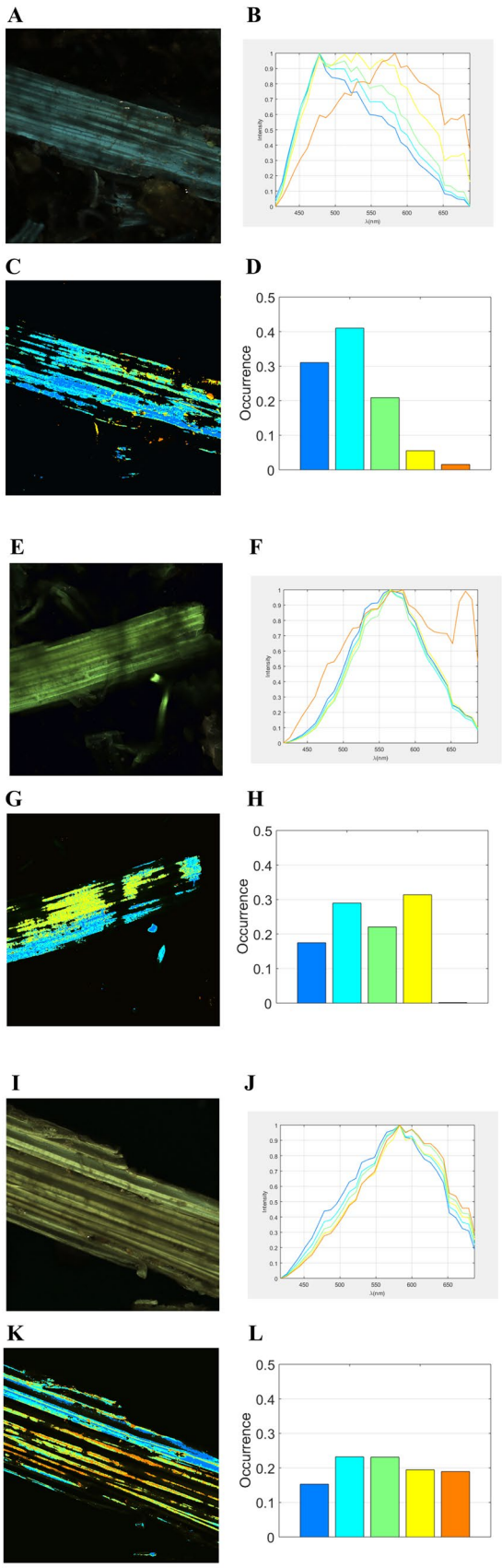

Fig. 3 Confocal laser scanning microscopy images and image processing results for untreated bagasse (**A**, **B**, **C**, **D**), alkali-pretreated SCB (**E**, **F**, **G**, **H**), and hydrothermal pretreated SCB (**I**, **J**, **K**, **L**) ▶

the native plant biomass and changes in lignin interactions imposed by delignifying pretreatments (Coletta et al., 2013; Espirito Santo et al., 2018; Paës, 2014). The absorption cross section of two-photon excitations is larger for molecular aggregates than for isolated lignin molecules. This confers a more selective excitation of condensed and aggregated lignin assemblies. Furthermore, molecular aggregates present intermolecular interactions such as hydrogen bonds and van der Walls forces that energetically disturb the electronic states of the lignin molecules that compose the aggregates. Such interactions, even if weak, produce a strong energetic broadening and a shift of the density of molecular states affecting their optical properties mainly in the region of lower energies. These new low-energy fluorescent states can be accessed by optical excitation via energy transfer mechanism followed by energy relaxation.

Previous confocal microscopy results suggest that lignin in native SCB is organized in the microscopic environments, stabilized by molecular interactions of lignin with hemicellulose and other biopolymers of the plant cell wall (Coletta et al., 2013; Espirito Santo et al., 2018). The thermochemical pretreatments disrupt natural organization of plant cell walls, which could lead to the formation of lignin aggregates and/or lignin degradation and solubilization (Brar et al., 2020; Coletta et al., 2013; Espirito Santo et al., 2018).

Here, we applied spectral CLSM to identify and characterized changes in the molecular organization of lignin within the SCB cell walls promoted by applied pretreatments. Three high-contrast CLSM images acquired in spectral mode of native, hydrothermally, and alkaline-pretreated SCB samples are given in Fig. 3A, E, and I, respectively. The samples were excited by two photons at 800 nm wavelength (1.54 eV) which produces optical transitions with the energy of around 3.1 eV (~400 nm, ultraviolet region). To ensure homogeneous spreading and horizontal deposition on a microscopic glass slide, the images were obtained on wet samples with the same field of view of $400 \times 400\ \mu m^2$ (1024×1024 pixels). The colors in the images in Fig. 3 A, E, and I result from an RGB decomposition of the measured spectrum for each image pixel in the visible region between 400 and 700 nm.

Therefore, changes in the color of each SCB fragments in the spectral images faithfully reflect relative variations in the intensities of the emission bands or eventual band shifts. Multivariance statistical analysis was applied to obtain additional information contained in the CLSM spectral images. Similar spectra were grouped into clusters, of which five most representative spectra were classified. Five

most representative spectral classes for each image are given in Fig. 3B, F, and J, and their relative weights are given in Fig. 3C, H, and L. It is clear that applied pretreatments modify lignin autofluorescence by shifting resulting autofluorescence spectra to red and enriching long-wavelength associated spectral classes (Fig. 3). Predominant spectral classes in the native SCB samples are associated with the lignin autofluorescence emission in blue and dark-blue region (Fig. 3B). Hydrothermal pretreatment leads to considerable spectral redistribution, with almost equal contributions from spectral classes associated with dark-blue, blue, green, and yellow emission (Fig. 3H), whereas alkaline pretreatment further adds red spectral component to it, revealing changes in the lignin organization (Fig. 3L).

The spectral classes demonstrate a decrease in the intensity of the bands associated with native, non-modified lignin (blue and dark blue) with simultaneous increase in the intensity and the spectral shift to the band associated with modified and possibly aggregated lignin (yellow and red). This indicates that an increase of modified lignin fraction results from the reduction of the native, non-modified lignin in the process of pretreatments. Thus, the observed changes in the fluorescence emission related to modified lignin are due to the increase in a number of the modified lignin species as well as to the broadening of the density of lignin states due to the higher diversity of molecular interactions in the modified lignin fraction. These two effects enhance electron migration processes and energetic relaxation of the excited state to lower energy-emitting states in the lignin aggregates, resulting in the observed spectral changes of the lignin autofluorescence emission.

Furthermore, alkaline pretreatment leads to more heterogeneously emitting samples, presumably resulting from chemical modifications of lignin and its heterogeneous solubilization and removal from the pretreated samples into solution (compare Fig. 3G, K).

X-Ray Powder Diffraction

Efficiency of enzymatic hydrolysis of plant biomass can be strongly impacted by the recalcitrance and crystallinity of the biomass samples (Espirito Santo et al., 2018). The crystallinity could be significantly impacted by the applied pretreatments, and for this reason we decided to determine crystallinity indices (CrIs) and the average size of the crystallites of raw and pretreated bagasse samples using X-ray powder diffraction (XRD; Fig. 4).

The CrIs of alkaline-pretreated sugar cane bagasse samples were significantly different from original, untreated SCB (Fig. 4). Comparison of chemical composition analysis of SCB samples (Fig. 2) and their crystallinity indices (Fig. 4) shows that the changes in SCB samples crystallinities were primarily due to removal of lignin fractions, caused by pretreatments. Hydrothermal pretreatment which did not result in strong lignin removal (Fig. 2) did not result in considerable changes in CrIs

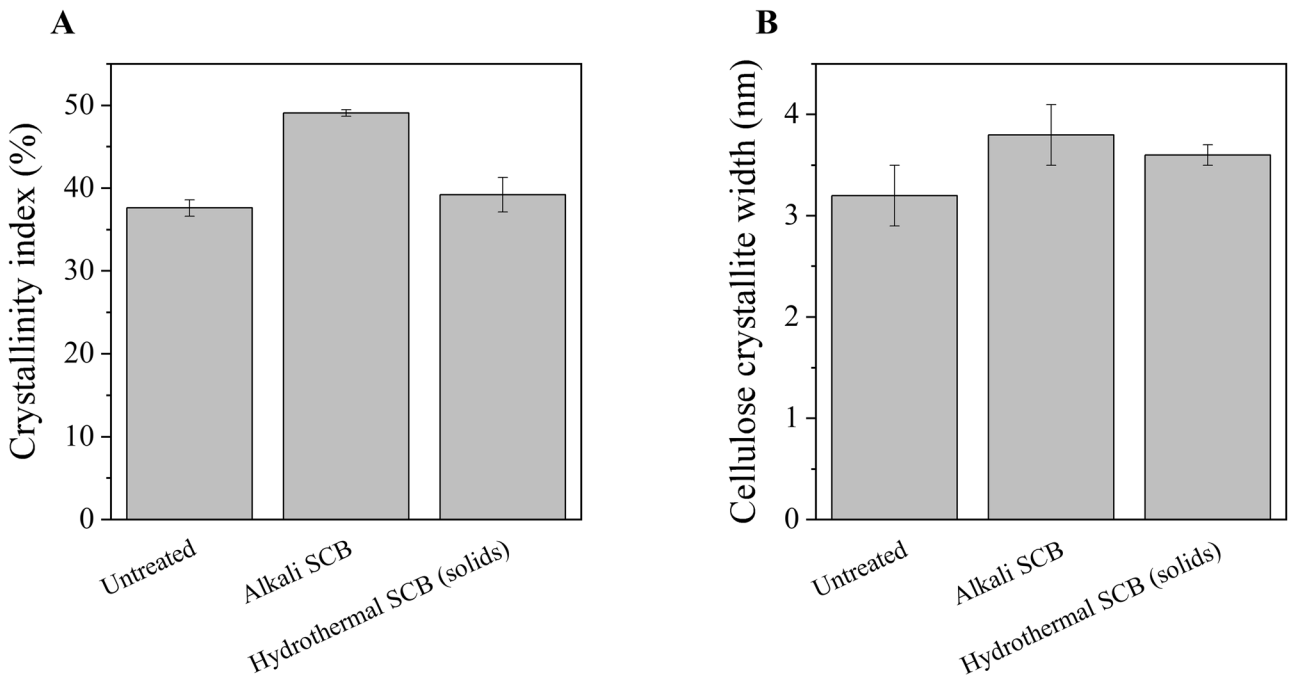

Fig. 4 Crystallinity index (**A**) and cellulose crystallite width (**B**) of untreated and pretreated solid residues from alkali and hydrothermal pretreatment on sugarcane bagasse. Results are expressed as mean ± standard deviation of triplicates ($n = 3$)

Table 1 Fractions of the biomass component that were transferred to the liquor after applied alkaline and hydrothermal pretreatments

Component	Alkali pretreatment	Hydrothermal pretreatment
Glucan	15%	15%
Xylan	37%	57%
Acetyl groups	100%	59%
Total lignin	74%	27%

for hydrothermally pretreated samples. Indeed, CrIs estimates based on the Segal equation (Fig. 4) agree well with the decrease in lignin contents of the pretreated samples (Fig. 2). Lignin and also partial hemicellulose removal allow for direct interfacing between cellulose crystallites, enabling co-crystallization and hornification of the resulting samples that have larger crystallites and higher crystallinities. This notion is in line with our results (Fig. 4), which reveal that the applied alkaline pretreatments resulted in higher CrIs and larger crystallites. Both CrIs and the average crystallite sizes were larger for alkaline-pretreated SCB samples, presumably because of the strong and heterogeneous removal of lignin, as demonstrated by CSLM images (Fig. 3) and chemical composition analyses (Fig. 2). Hydrothermal pretreatment resulted in the samples with smaller CrIs and average crystallite sizes, which were closer to the raw SCB samples (Fig. 4), which is in line with CLSM analyses (Fig. 3). This also indicates that lignin removal was crucial for observed changes in CrIs and the average crystallite sizes.

XOS Production During Biomass Pretreatments

Taking into consideration the chemical composition of the solid fractions, shown in Fig. 2, as well as the solids recoveries, we were able to calculate the fraction of the initial mass of each constituent that was transferred to the liquor in the pretreatments (Table 1). As an example, from the total lignin found in the untreated bagasse, 74% was found in the liquid fraction after alkali pretreatment, while the other 26% remained in the solid fraction. The opposite happens after hydrothermal pretreatment: 27% of the initial lignin was transferred in the liquor, while the other 73% remained in the solid fraction. Although the values of hydrothermal pretreatment mass transfer to liquor are higher than those previously reported by Santucci et al. (2015) for that same condition (160 °C, 60 min), it should be pointed out that their mass recovery was higher than the one we achieved.

In order to quantify a part of the xylan that was solubilized in the form of XOS in the resulting pretreatment liquors, the liquid fraction, resulting from biomass hydrothermal pretreatments alone, was analyzed using HPAEC. Figure 5 shows HPAEC profile and XOS concentrations in the liquid fraction obtained after pretreatments.

It is clear that alkali pretreatment alone did not yield appreciable quantities of XOS in the soluble fraction, while hydrothermal pretreatment produced wide range of XOS with different degrees of polymerization, resulting in approximately 1 mg/mL of functional XOS (X2–X6) plus the unidentified oligosaccharides with the retention times greater than that of X6, which might correspond to longer XOS (X7, X8, X9) and/or to decorated arabino-XOS

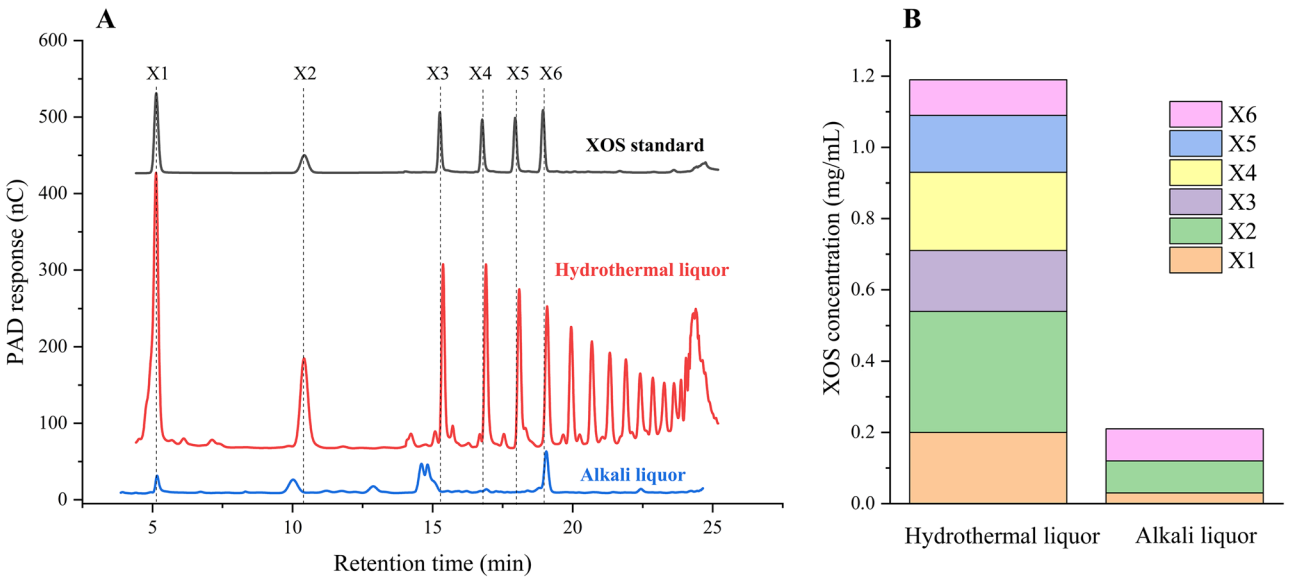

Fig. 5 XOS production from pretreatments alone. **A** HPAEC profile from alkali and hydrothermal liquor; **B** XOS yields, in mg per mL of liquor, after pretreatment application

(Bhattacharya et al., 2020). This is consistent with the notion that alkali pretreatment mainly leads to degradation of lignin and partial hemicellulose removal, whereas considerable hemicellulose solubilization and partial depolymerization occurs during hydrothermal pretreatment. Furthermore, it elucidates the potential of enzymatic hydrolysis of the hydrothermal liquor to transform long oligomers into short XOS, which have better prebiotic properties, improving their yields (Singh et al., 2015).

Enzymatic Hydrolysis

Three different enzymes endo-β-xylanases *Px*Xyn10A and *Px*Xyn11B and a novel metagenomics xylobiohydrolase MetXyn11 identified in a microbial consortium were applied to liquid and solid fractions of the hydrothermally pretreated biomass samples and solids after alkaline pretreatment. After applying different enzyme combinations to biomass samples, XOS and xylose yields and profiles were analyzed (Fig. 6). Enzymatic hydrolysis of untreated SCB was also performed and did not result in any detectable XOS production (data not shown).

The enzymatic hydrolysis on SCB-Alk substrate with xylanases produced X4 as the longest quantifiable oligomer and X2 as the main product. This shows that endo-xylanases were indeed capable of depolymerizing xylan into its smallest oligomers. Since SCB-Alk was completely deacetylated by the alkaline pretreatment (Fig. 2), the obtained XOS are also fully deacetylated.

In contrast, hydrothermally pretreated SCB, an acetylated substrate, provided quantifiable XOS with DP up to 6. X2 and X3 were the main components obtained by the enzymatic hydrolysis of the solid pretreated fraction, while liquor hydrolysate contains mostly X2, as well as X1 and X3 as main components.

Although considered an undesired product due to its lower prebiotic activity and potential inhibitory effects, xylose, which originates from the pretreatment process and/or from hydrolysis by xylanases, has been used as feedstock for other biotechnological applications, such as xylitol production (Zhang, Ren et al., 2021; Zhang, Han et al., 2021). For all the substrates, except for the liquor hydrolysate, hydrolysis by GH11 xylanase alone contain little or no detectable amount of xylose, compatible with the product profile of this family of enzymes. The presence of xylose in the liquor hydrolysate can be explained by the fact that there is xylose in the non-hydrolyzed liquor (sample 0:0); therefore, it is likely to be not a product of GH11 xylanase, but rather a product from the pretreatment. It is interesting to note that, in general, the greater GH10:GH11 ratio, the lower the proportion of longer XOS is found in the hydrolysate. This is in line with the fact that GH10 xylanases tend to provide shorter oligomers than GH11 members as the hydrolytic products (Maslen et al., 2007; Srivastava et al., 2020). For all the substrates, the hydrolysates of GH11 alone contain little or no detectable amount of xylose, compatible with the product profile of this family of enzymes, except for the liquor hydrolysate. However, this can be explained by the fact that there is xylose in the non-hydrolyzed liquor (sample 0:0); therefore, it is not a product of the xylanase, but rather a product from the pretreatment. Additionally, *Px*Xyn10A alone accomplished the highest XOS yields on all three substrates, while MetXyn11 alone was the least effective on all studied substrates, probably due to its xylobiohydrolase character (Evangelista et al., 2019; Kadowaki et al., 2021).

The best experimentally obtained yield was 47.6 ± 0.2 mg of XOS/g of untreated biomass with enzymatic hydrolysis in SCB-Alk, which does not include xylose. For SCB-HT and SCB-HT-Liq, the figures were 14.5 ± 0.1 mg/g and 81 ± 1 mg/g, respectively. Concerning the liquid fraction,

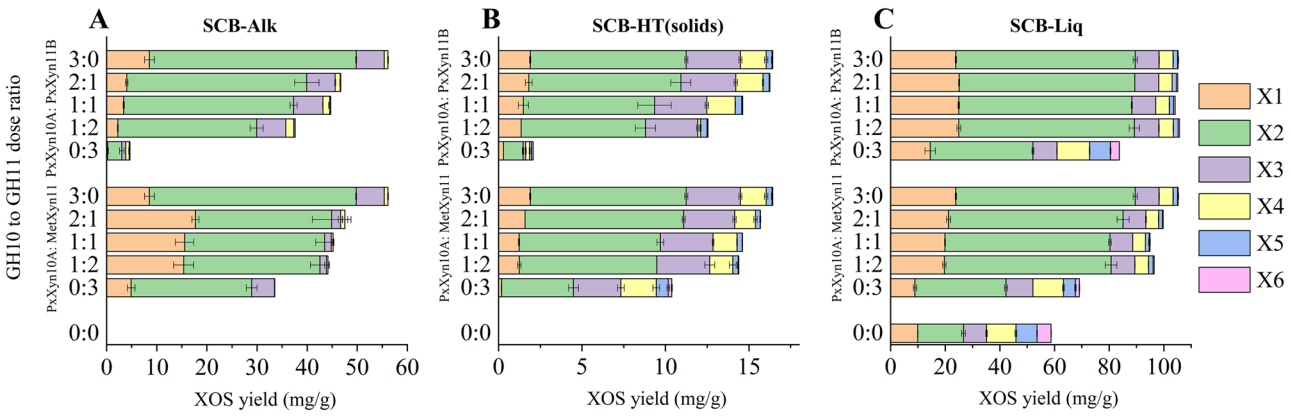

Fig. 6 XOS and xylose yields (in mg/g initial biomass) with different enzyme combinations against alkali (**A**) and hydrothermal (solid (**B**) and liquor (**C**) fractions) pretreated sugarcane bagasse in 2% (w/v) reactions for solid substrates and 33% (v/v) reactions on SCB-HT-Liq. Condition 0:0 represents a sample that was not enzymatically hydrolyzed

enzymatic hydrolysis was able to enhance in around 67% the yield of functional XOS as compared to non-hydrolyzed liquor. In spite of its low xylan proportion, due to efficient xylan solubilization in hydrothermal pretreatment, enzymatic hydrolysis on SCB-HT could improve total hydrothermal path yield in 17.9%, thus resulting in a total yield of 96 ± 1 mg/g when combining XOS yields from solid and liquid fractions of hydrothermally pretreated SCB.

These results are consistent with the crystallinity indexes given in Fig. 4, since the materials with lower CrIs presented lower hydrolysis yields (untreated and hydrothermally pretreated SCB solids), whereas SCB-Alk, which resulted in the best yields among the solid substrates, had higher CrI as compared to the untreated biomass. Therefore, there is a positive correlation between CrI and the enzymatic hydrolysis yield: the higher the CrI, the higher the yields of xylan from enzymatic hydrolysis. This can be explained by the fact that alkaline pretreatment mostly solubilizes and removes amorphous lignin, thus disrupting the recalcitrant lignocellulosic matrix and facilitating access of enzymes to hemicellulose. Simultaneously, the removal of lignin and cellulose hornification and partial crystallization reveal themselves in an increase in CrI and an increase in the average cellulose crystallite size of the alkaline-pretreated solids (Fig. 4). This does not happen in the course of hydrothermal pretreatment which mostly solubilizes xylan, while the lignin fraction predominantly remains in the pretreated solids (Table 1).

Considering that about 20% of SCB xylopyranose residues bear L-arabinose decorations (Campbell et al., 2019) which will make them and the two consecutive non-decorated residues not accessible to enzymatic hydrolysis, the best enzymatically-produced XOS yields are probably close to the highest possible theoretical yield which can be obtained with GH10 xylanases. Therefore, the use of α-L-arabinofurosidases (EC 3.2.1.55) might be necessary to remove arabinoxylan decorations aiming to further increase XOS yields (Xue et al., 2023).

Data of XOS yield after enzymatic hydrolysis on SCB liquor with xylanases is still scarce in literature; however, similar processes have already been performed using dilute acid or hydrothermal pretreatments, however leading to different XOS lengths distributions. The published yields are quite comparable to the ones obtained in this study. de Figueiredo and collaborators (2017), for instance, were able to obtain 32 mg of XOS per gram of initial biomass by pretreating SCB with 5% KOH, for 30 min at 121 °C and then applying an endoxylanase from *Aspergillus fumigatus* M51. As for hydrothermal treatment, Zhang et al. (2018) could obtain 71 mg/g from 60 min of pretreatment at 160 °C and Carvalho et al. (2018) were able to achieve 82 mg/g in a short pretreatment (5 min at 190 °C) catalyzed with 0.5% sulfuric acid.

Recent studies could achieve better overall yields (Zhao et al., 2021; Zhou & Xu, 2019) via diluted acid hydrolysis with acetic and phosphoric acids. However, external load of acids was avoided in our experiments in order to explore the potential of acetyl groups naturally present in the hemicellulose fraction (2.32% of bagasse dry mass) as a catalyst for xylan solubilization during hydrothermal pretreatment. Moreover, detailed comparison of XOS profiles generated by different enzymatic mixtures of GH10 and GH11 xylanases and GH11 xylobiohydrolase conducted in present study can serve as a basis for further optimization of enzymatic XOS production.

Conclusions

This work aimed to compare two different pretreatment routes for XOS production from sugarcane bagasse, while also assessing the potential synergistic effect between xylanases from families GH10 and GH11 and a recently described xylobiohydrolase. From the XOS production paths evaluated in this study, hydrothermal pretreatment followed by enzymatic hydrolysis of liquid fraction rendered nearly twice as much XOS when compared to enzymatic hydrolysis on solid fraction of alkali-pretreated SCB. Concerning the use of different enzyme combinations, it became clear that the degree of substitution of sugarcane xylan can be an obstacle in xylan hydrolysis with GH11 xylanases, as the hydrolysis with GH10 xilanase alone yielded higher quantities of XOS for all the tested substrates. Furthermore, while the hydrothermal liquor itself contains considerable amounts of XOS, the benefit of an enzymatic hydrolysis step is in considerable improvement of short-length, functional, XOS yields. Under studied conditions, hydrothermal pretreatment, that alone could produce around 48.8 mg of short XOS per gram of untreated bagasse, was further busted by almost two times after enzymatic treatment of both solid and liquid fractions. The later strategy was the most efficient in the context of functional XOS production. It might represent a promising "green" route for agricultural by-products value enhancement with minimum ecological impacts.

Author Contribution Caio Cesar de Mello Capetti: designed research, performed research, analyzed data, and wrote the paper. Vanessa de Oliveira Arnoldi Pellegrini: designed research, performed research, analyzed data, and wrote the paper. Milena Moreira Vacilotto: performed research and analyzed data. Antonio Aprigio da Silva Curvelo: designed research, performed research, analyzed data, and wrote the paper. Maurício Falvo: conducted CSLM data analysis and wrote the paper. Francisco Eduardo Gontijo Guimaraes: performed research and conducted CSLM data acquisition. Ornella M. Ontañon: performed research. Eleonora Campos: designed research, performed research, acquired funding, and wrote the paper. Igor Polikarpov: designed research, analyzed data, wrote the paper, and acquired funding.

Funding This research was supported by Fundação de Amparo à Pesquisa do Estado de São Paulo (FAPESP, São Paulo, Brazil) via grants 2019/10942–0 (to CC) and 2021/08780–1 (to IP), by the Conselho Nacional de Desenvolvimento Científico e Tecnológico (CNPq, Brazil: grants 306852/2021–7 and 440180/2022–8, to IP), and by the Agencia Nacional de Promoción de la Investigación (Argentina, grant PICT CABBIO 2016–4695, to EC).

Data Availability The authors declare that the data supporting the findings of this study are available within the paper and its Supplementary Information files. Should any raw data files be needed in another format they are available from the corresponding author upon reasonable request.

Declarations

Conflict of Interest The authors declare no competing interests.

References

Alekhina, M., Mikkonen, K. S., Alén, R., Tenkanen, M., & Sixta, H. (2014). Carboxymethylation of alkali extracted xylan for preparation of bio-based packaging films. *Carbohydrate Polymers, 100*, 89–96. https://doi.org/10.1016/j.carbpol.2013.03.048

Asahara, T., Nomoto, K., Shimizu, K., Watanuki, M., & Tanaka, R. (2001). Increased resistance of mice to salmonella enterica serovar typhimurium infection by synbiotic administration of bifidobacteria and transgalactosylated oligosaccharides. *Journal of Applied Microbiology, 91*(6), 985–996. https://doi.org/10.1046/j.1365-2672.2001.01461.x

Bhattacharya, A., Ruthes, A., Vilaplana, F., Karlsson, E. N., Adlecreutz, P., & Stålbrand, H. (2020). Enzyme synergy for the production of arabinoxylo-oligosaccharides from highly substituted arabinoxylan and evaluation of their prebiotic potential. *LWT, 131*, 109762. https://doi.org/10.1016/j.lwt.2020.109762

Biely, P., Singh, S., & Puchart, V. (2016). Towards enzymatic breakdown of complex plant xylan structures: State of the art. *Biotechnology Advances, 34*(7), 1260–1274. https://doi.org/10.1016/j.biotechadv.2016.09.001

Brar, K. K., Espirito Santo, M. C., Pellegrini, V. O. A., deAzevedo, E. R., Guimaraes, F. E. C., Polikarpov, I., & Chadha, B. S. (2020). Enhanced hydrolysis of hydrothermally and autohydrolytically treated sugarcane bagasse and understanding the structural changes leading to improved saccharification. *Biomass and Bioenergy, 139*(June), 105639. https://doi.org/10.1016/j.biombioe.2020.105639

Campbell, G. M., Čukelj Mustač, N., Alyassin, M., Gomez, L. D., Simister, R., Flint, J., et al. (2019). Integrated processing of sugarcane bagasse: Arabinoxylan extraction integrated with ethanol production. *Biochemical Engineering Journal, 146*, 31–40. https://doi.org/10.1016/j.bej.2019.03.001

Capetti, C. C. de M., Vacilotto, M. M., Dabul, A. N. G., Sepulchro, A. G. V., Pellegrini, V. O. A., & Polikarpov, I. (2021). Recent advances in the enzymatic production and applications of xylo-oligosaccharides. *World Journal of Microbiology and Biotechnology*, *37*(10), 1–12. https://doi.org/10.1007/S11274-021-03139-7

Carvalho, A. F. A., Marcondes, W. F., de Oliva Neto, P., Pastore, G. M., Saddler, J. N., & Arantes, V. (2018). The potential of tailoring the conditions of steam explosion to produce xylo-oligosaccharides from sugarcane bagasse. *Bioresource Technology*, *250*(November 2017), 221–229. https://doi.org/10.1016/j.biortech.2017.11.041

Coletta, V. C., Rezende, C. A., da Conceição, F. R., Polikarpov, I., & Guimarães, F. E. G. (2013). Mapping the lignin distribution in pretreated sugarcane bagasse by confocal and fluorescence lifetime imaging microscopy. *Biotechnology for Biofuels, 6*(1), 43. https://doi.org/10.1186/1754-6834-6-43

CONAB (Companhia Nacional de Abastecimento). (2021). *Acompanhamento da safra brasileira de cana-de-açúcar*. Available from: https://www.conab.gov.br/info-agro/safras/cana. Accessed 29 Aug 2021

Costa, J. M., Strieder, M. M., Saldaña, M. D. A., Rostagno, M. A., & Forster-Carneiro, T. (2023). Recent advances in the processing of agri-food by-products by subcritical water. *Food and Bioprocess Technology*. https://doi.org/10.1007/s11947-023-03071-8

de Capetti, C. C. M., Nicoli, A., Dabul, G., Oliveira, V. De, Pellegrini, A., & Polikarpov, I. (2023). *Chapter 13 - Mannanases and other mannan-degrading enzymes*. Elsevier Inc. https://doi.org/10.1016/B978-0-323-91805-3.00013-7

de Carvalho, D. M., de Queiroz, J. H., & Colodette, J. L. (2016). Assessment of alkaline pretreatment for the production of bioethanol from eucalyptus, sugarcane bagasse and sugarcane straw. *Industrial Crops and Products, 94*, 932–941. https://doi.org/10.1016/j.indcrop.2016.09.069

de Castro, R. C., & A., Fonseca, B. G., dos Santos, H. T. L., Ferreira, I. S., Mussatto, S. I., & Roberto, I. C. (2017). Alkaline deacetylation as a strategy to improve sugars recovery and ethanol production from rice straw hemicellulose and cellulose. *Industrial Crops and Products, 106*, 65–73. https://doi.org/10.1016/j.indcrop.2016.08.053

de Figueiredo, F. C., Carvalho, A. F. A., Brienzo, M., Campioni, T. S., & de Oliva-Neto, P. (2017). Chemical input reduction in the arabinoxylan and lignocellulose alkaline extraction and xylooligosaccharides production. *Bioresource Technology, 228*, 164–170. https://doi.org/10.1016/j.biortech.2016.12.097

de Freitas, C., Carmona, E., & Brienzo, M. (2019). Xylooligosaccharides production process from lignocellulosic biomass and bioactive effects. *Bioactive Carbohydrates and Dietary Fibre*, *18*(October 2018), 100184. https://doi.org/10.1016/j.bcdf.2019.100184

de Pellegrini, V., O. A., Ratti, R. P., Filgueiras, J. G., Falvo, M., Coral, M. A. L., Guimaraes, F. E. G., et al. (2022). Differences in chemical composition and physical properties caused by industrial storage on sugarcane bagasse result in its efficient enzymatic hydrolysis. *Sustainable Energy & Fuels, 6*(2), 329–348. https://doi.org/10.1039/D1SE01240A

de Souza, T. S. P., & Kawaguti, H. Y. (2021). Cellulases, hemicellulases, and pectinases: Applications in the food and beverage industry. *Food and Bioprocess Technology, 14*(8), 1446–1477. https://doi.org/10.1007/s11947-021-02678-z

Deutschmann, R., & Dekker, R. F. H. (2012). From plant biomass to bio-based chemicals: Latest developments in xylan research. *Biotechnology Advances, 30*(6), 1627–1640. https://doi.org/10.1016/j.biotechadv.2012.07.001

Espirito Santo, M., Rezende, C. A., Bernardinelli, O. D., Pereira, N., Curvelo, A. A. S., deAzevedo, E. R., et al. (2018). Structural and compositional changes in sugarcane bagasse subjected to hydrothermal and organosolv pretreatments and their impacts on enzymatic hydrolysis. *Industrial Crops and Products, 113*(January), 64–74. https://doi.org/10.1016/j.indcrop.2018.01.014

Evangelista, D. E., & de Oliveira Arnoldi Pellegrini, V., Santo, M. E., McQueen-Mason, S., Bruce, N. C., & Polikarpov, I. (2019). Biochemical characterization and low-resolution SAXS shape of a novel GH11 exo-1,4-β-xylanase identified in a microbial consortium. *Applied Microbiology and Biotechnology, 103*(19), 8035–8049. https://doi.org/10.1007/s00253-019-10033-8

Farhat, W., Venditti, R., Quick, A., Taha, M., Mignard, N., Becquart, F., & Ayoub, A. (2017). Hemicellulose extraction and characterization for applications in paper coatings and adhesives. *Industrial Crops and Products, 107*, 370–377. https://doi.org/10.1016/j.indcrop.2017.05.055

Forgy, E. W. (1965). Cluster analysis of multivariate data - Efficiency vs interpretability of classifications. *Biometrics, 21*(3), 768.

Ghio, S., Ontañon, O., Piccinni, F. E., Marrero Díaz de Villegas, R., Talia, P., Grasso, D. H., & Campos, E. (2018). *Paenibacillus* sp. A59 GH10 and GH11 extracellular endoxylanases: Application in biomass bioconversion. *Bioenergy Research*, *11*(1), 174–190. https://doi.org/10.1007/s12155-017-9887-7

Gouveia, E. R., Nascimento, R. T. D., Souto-Maior, A. M., & de Rocha, G. J. M. (2009). Validação de metodologia para a caracterização química de bagaço de cana-de-açúcar. *Quimica Nova, 32*(6), 1500–1503. https://doi.org/10.1590/S0100-40422009000600026

Gufe, C., Ngenyoung, A., Rattanarojpong, T., & Khunrae, P. (2022). Investigation into the effects of CbXyn10C and Xyn11A on xylooligosaccharide profiles produced from sugarcane bagasse and rice straw and their impact on probiotic growth. *Bioresource Technology, 344*, 126319. https://doi.org/10.1016/j.biortech.2021.126319

Hitache, Z., Al-Dalali, S., Pei, H., & Cao, X. (2023). Review of the health benefits of cereals and pseudocereals on human gut microbiota. *Food and Bioprocess Technology*, (0123456789). https://doi.org/10.1007/s11947-023-03069-2

Hong, K. B., Kim, J. H., Kwon, H. K., Han, S. H., Park, Y., & Suh, H. J. (2016). Evaluation of prebiotic effects of high-purity galactooligosaccharides in vitro and in vivo. *Food Technology and Biotechnology*, *54*(2). https://doi.org/10.17113/ftb.54.02.16.4292

Kadowaki, M. A. S., Briganti, L., Evangelista, D. E., Echevarría-Poza, A., Tryfona, T., Pellegrini, V. O. A., et al. (2021). Unlocking the structural features for the xylobiohydrolase activity of an unusual GH11 member identified in a compost-derived consortium. *Biotechnology and Bioengineering, 118*(10), 4052–4064. https://doi.org/10.1002/bit.27880

Ma, L., Crawford, M. M., & Tian, J. (2010). Local manifold learning-based k -nearest-neighbor for hyperspectral image classification. *IEEE Transactions on Geoscience and Remote Sensing*. https://doi.org/10.1109/TGRS.2010.2055876

Malgas, S., Mafa, M. S., Mkabayi, L., & Pletschke, B. I. (2019). A mini review of xylanolytic enzymes with regards to their synergistic interactions during hetero-xylan degradation. *World Journal of Microbiology and Biotechnology, 35*(12), 187. https://doi.org/10.1007/s11274-019-2765-z

Maslen, S. L., Goubet, F., Adam, A., Dupree, P., & Stephens, E. (2007). Structure elucidation of arabinoxylan isomers by normal phase HPLC-MALDI-TOF/TOF-MS/MS. *Carbohydrate Research, 342*(5), 724–735. https://doi.org/10.1016/j.carres.2006.12.007

Mello, B. L., Alessi, A. M., Riaño-Pachón, D. M., DeAzevedo, E. R., Guimarães, F. E. G., Espirito Santo, M. C., et al. (2017). Targeted metatranscriptomics of compost-derived consortia reveals a GH11 exerting an unusual exo-1,4-β-xylanase activity. *Biotechnology for Biofuels, 10*(1), 254. https://doi.org/10.1186/s13068-017-0944-4

Monshi, A., Foroughi, M. R., & Monshi, M. R. (2012). Modified Scherrer equation to estimate more accurately nano-crystallite size using XRD. *World Journal of Nano Science and Engineering, 02*(03), 154–160. https://doi.org/10.4236/wjnse.2012.23020

Paës, G. (2014). Fluorescent probes for exploring plant cell wall deconstruction: A review. *Molecules, 19*(7), 9380–9402. https://doi.org/10.3390/molecules19079380

Poletto, P., Pereira, G. N., Monteiro, C. R. M., Pereira, M. A. F., Bordignon, S. E., & de Oliveira, D. (2020). Xylooligosaccharides: Transforming the lignocellulosic biomasses into valuable 5-carbon sugar prebiotics. *Process Biochemistry*, *91*(December 2019), 352–363. https://doi.org/10.1016/j.procbio.2020.01.005

Rezende, C., de Lima, M., Maziero, P., DeAzevedo, E., Garcia, W., & Polikarpov, I. (2011). Chemical and morphological characterization of sugarcane bagasse submitted to a delignification process for enhanced enzymatic digestibility. *Biotechnology for Biofuels, 4*(1), 54. https://doi.org/10.1186/1754-6834-4-54

Ruiz, H. A., Rodríguez-Jasso, R. M., Fernandes, B. D., Vicente, A. A., & Teixeira, J. A. (2013). Hydrothermal processing, as an alternative for upgrading agriculture residues and marine biomass according to the biorefinery concept: A review. *Renewable and Sustainable Energy Reviews, 21*, 35–51. https://doi.org/10.1016/j.rser.2012.11.069

Santibáñez, L., Henríquez, C., Corro-Tejeda, R., Bernal, S., Armijo, B., & Salazar, O. (2021). Xylooligosaccharides from lignocellulosic biomass: A comprehensive review. *Carbohydrate Polymers*, *251*(September 2020), 117118. https://doi.org/10.1016/j.carbpol.2020.117118

Santucci, B. S., Maziero, P., Rabelo, S. C., Curvelo, A. A. S., & Pimenta, M. T. B. (2015). Autohydrolysis of hemicelluloses from sugarcane bagasse during hydrothermal pretreatment: A kinetic assessment. *Bioenergy Research, 8*(4), 1778–1787. https://doi.org/10.1007/s12155-015-9632-z

Scapini, T., dos Santos, M. S. N., Bonatto, C., Wancura, J. H. C., Mulinari, J., Camargo, A. F., et al. (2021). Hydrothermal pretreatment of lignocellulosic biomass for hemicellulose recovery. *Bioresource Technology, 342*, 126033. https://doi.org/10.1016/J.BIORTECH.2021.126033

Scherrer, P. (1912). Bestimmung der inneren Struktur und der Größe von Kolloidteilchen mittels Röntgenstrahlen. In *Kolloidchemie Ein Lehrbuch* (pp. 387–409). Berlin, Heidelberg: Springer Berlin Heidelberg. https://doi.org/10.1007/978-3-662-33915-2_7

Segal, L., Creely, J. J., Martin, A. E., & Conrad, C. M. (1959). An empirical method for estimating the degree of crystallinity of native cellulose using the X-ray diffractometer. *Textile Research Journal, 29*(10), 786–794. https://doi.org/10.1177/004051755902901003

Singh, R. D., Banerjee, J., & Arora, A. (2015). Prebiotic potential of oligosaccharides: A focus on xylan derived oligosaccharides. *Bioactive Carbohydrates and Dietary Fibre, 5*(1), 19–30. https://doi.org/10.1016/j.bcdf.2014.11.003

Sluiter, A., Hames, B., Ruiz, R., Scarlata, C., Sluiter, J., & Templeton, D. (2008a). *Determination of ash in biomass*. www.nrel.gov

Sluiter, A., Hames, B., Ruiz, R., Scarlata, C., Sluiter, J., Templeton, D., & Crocker, D. (2008b). Determination of structural carbohydrates and lignin in biomass. In *National Renewable Energy Laboratory* (NREL/ TP-510-42618) (Issue January). http://www.nrel.gov/biomass/pdfs/42618.pdf

Srivastava, N., Mishra, P. K., & Upadhyay, S. N. (2020). Xylanases: For digestion of hemicellulose. In *Industrial Enzymes for Biofuels Production* (pp. 101–132). Elsevier. https://doi.org/10.1016/B978-0-12-821010-9.00006-1

Timell, T. E. (1967). Recent progress in the chemistry of wood hemicelluloses. *Wood Science and Technology, 1*(1), 45–70. https://doi.org/10.1007/BF00592255

Vázquez, M. J., Alonso, J. L., Domínguez, H., & Parajó, J. C. (2000). Xylooligosaccharides: Manufacture and applications. *Trends in Food Science and Technology, 11*(11), 387–393. https://doi.org/10.1016/S0924-2244(01)00031-0

Vieira, T. F., Corrêa, R. C. G., Peralta, R. A., Peralta-Muniz-Moreira, R. F., Bracht, A., & Peralta, R. M. (2020). An overview of structural aspects and health beneficial effects of antioxidant oligosaccharides. *Current Pharmaceutical Design, 26*(16), 1759–1777. https://doi.org/10.2174/1381612824666180517120642

Wang, W., Yuan, T., Wang, K., Cui, B., & Dai, Y. (2012). Combination of biological pretreatment with liquid hot water pretreatment to enhance enzymatic hydrolysis of *Populus tomentosa*. *Bioresource Technology, 107*, 282–286. https://doi.org/10.1016/j.biortech.2011.12.116

Wu, W., Jiao, A., Xu, E., Chen, Y., & Jin, Z. (2020). Effects of extrusion technology combined with enzymatic hydrolysis on the structural and physicochemical properties of porous corn starch. *Food and Bioprocess Technology, 13*(3), 442–451. https://doi.org/10.1007/s11947-020-02404-1

Xue, Y., Song, Y., Wu, J., Gan, L., Long, M., & Liu, J. (2023). Characterization of the recombinant GH10 xylanase from *Trichoderma*

orientalis EU7-22 and its synergistic hydrolysis of bamboo hemicellulose with α-glucuronidase and α-L-arabinofuranosidase. *Industrial Crops and Products, 194*, 116330. https://doi.org/10.1016/j.indcrop.2023.116330

Yuansah, S. C., Laga, A., & Pirman. (2023). Production strategy of functional oligosaccharides from lignocellulosic biomass using enzymatic process: A review. *Food and Bioprocess Technology*. https://doi.org/10.1007/s11947-023-03063-8

Zhang, B., Ren, L., Zhao, Z., Zhang, S., Xu, D., Zeng, X., & Li, F. (2021). High temperature xylitol production through simultaneous co-utilization of glucose and xylose by engineered *Kluyveromyces marxianus*. *Biochemical Engineering Journal, 165*, 107820. https://doi.org/10.1016/j.bej.2020.107820

Zhang, H., Han, L., & Dong, H. (2021). An insight to pretreatment, enzyme adsorption and enzymatic hydrolysis of lignocellulosic biomass: Experimental and modeling studies. *Renewable and Sustainable Energy Reviews, 140*, 110758. https://doi.org/10.1016/J.RSER.2021.110758

Zhang, W., You, Y., Lei, F., Li, P., & Jiang, J. (2018). Acetyl-assisted autohydrolysis of sugarcane bagasse for the production of xylo-oligosaccharides without additional chemicals. *Bioresource Technology, 265*, 387–393. https://doi.org/10.1016/j.biortech.2018.06.039

Zhao, S., Zhang, G. L., Chen, C., Yang, Q., Luo, X. M., Wang, Z. B., et al. (2021). A combination of mild chemical pre-treatment and enzymatic hydrolysis efficiently produces xylooligosaccharides from sugarcane bagasse. *Journal of Cleaner Production, 291*, 125972. https://doi.org/10.1016/J.JCLEPRO.2021.125972

Zhou, X., & Xu, Y. (2019). Integrative process for sugarcane bagasse biorefinery to co-produce xylooligosaccharides and gluconic acid. *Bioresource Technology, 282*, 81–87. https://doi.org/10.1016/j.biortech.2019.02.129

Zhu, Z., Rezende, C. A., Simister, R., McQueen-Mason, S. J., Macquarrie, D. J., Polikarpov, I., & Gomez, L. D. (2016). Efficient sugar production from sugarcane bagasse by microwave assisted acid and alkali pretreatment. *Biomass and Bioenergy, 93*, 269–278. https://doi.org/10.1016/j.biombioe.2016.06.017